Chapter 2

Baseline Detector

2.1 Introduction

In the Preliminary Conceptual Design Report (pCDR), "Standard" and "Basic" detector versions for the PHENIX experiment were defined. The Standard version addressed the full range of physics topics that the PHENIX collaboration would like to study. The Basic version was a particular subset of the Standard one that, based on preliminary cost estimates, could be built within the budget. It was shown in the pCDR that the Basic version could perform most of the PHENIX physics program.

In the present Conceptual Design Report (CDR) for the PHENIX experiment, the available budget was again confronted with considerably more refined cost estimates, and a detector configuration that can be built for Day-1 operation at RHIC was developed. Although this configuration is very similar to the Basic version, it is different in some details, and it is reffered to as the "Baseline" detector configuration. This chapter is devoted to a brief description of its component subsystems. The physics performance of the Baseline detector is discussed in Chapter 3. The detailed technical, cost, and schedule parameters of each subsystem are discussed in Chapters 4 through 11. In Chapter 15 a number of possible upgrades to the Baseline detector are discussed.

2.2 Coverage and Geometry

The PHENIX Baseline detector consists of three instrumented spectrometers or "arms". Two of these are centered at zero pseudorapidity ($\theta = 90°$) and are instrumented to detect electrons, photons, and charged hadrons. The two central arms are each $90°$ in ϕ but not exactly back-to-back, such that $\Delta\phi = 135°$. This arrangement lessens the nonuniformity in the p_T acceptance for the two arm configuration. The third spectrometer arm has full azimuthal coverage in the polar angle range $10° \leq \theta \leq 35°$, relative to the clockwise beam direction. The forward arm will detect muons. In addition to the three spectrometer arms, PHENIX has a detector subsystem, referred to as the "inner detectors", to measure and determine the start time, vertex, and multiplicity of an interaction. Table 2.1 summarizes the coverage of the central and forward arms, and the inner detectors.

Table 2.1: Angular and Pseudorapidity Coverage of PHENIX

Element	θ (deg.)	η	ϕ (deg.)	$\Delta\Omega$ (sr)
Central Arms	70–110	-0.35–0.35	$\pm$(22.5–112.5)	1.07
Forward Arm	10–35	1.15–2.44	0–360	1.17
Inner Detectors	2–178	-4.0–4.0	0–360	$\sim 4\pi$

2.3 Central Arms

The central arms are composed of detector elements that perform the functions of charged particle tracking and momentum measurement, electron and photon energy measurement, and particle identification. Table 2.2 summarizes the function and radial location of these elements. Figure 2.1 shows a cross-section of the central arm detector layout.

Table 2.2: Baseline Configuration: Central Arm Detectors

Element	Radial Space(mm)	Channel Count	Function
DC	2000–2475	10,240	Tracking and pattern recognition primarily in r-ϕ, momentum measurement.
PC1	2475–2525	15,000	Pattern recognition and tracking, primarily in z.
RICH	2575–4000	6400	Electron identification up to $p \approx 3$ GeV/c.
PC2	4050–4100	16,000	Pattern recognition and tracking, primarily in z.
TEC	4100–4800	29,000	Pattern recognition, tracking in r-ϕ, and electron identification by dE/dx up to $p \approx 2$ GeV/c.
PC3	4800–4850	16,000	Pattern recognition and tracking, primarily in z.
TOF	4900–5050	1000	Hadron identification, π/K up to 2.4 GeV/c.
EMCal	5100–6000	28,000	e/γ measurements by energy, shape, and timing. Electron identification below 350 MeV/c by time-of-flight and above 1 GeV/c by E-p matching. K/e separation up to 1 GeV/c by time-of-flight for dE/dx.

2.3.1 Charged Particle Tracking and Momentum Measurement

The collision point is surrounded by a central magnet (CM) that produces an axial field. The CM is described in Chapter 4. The design contains two sets of axial coils that provide many possible radial field distributions, including one with zero field at $r = 0$. In the Baseline

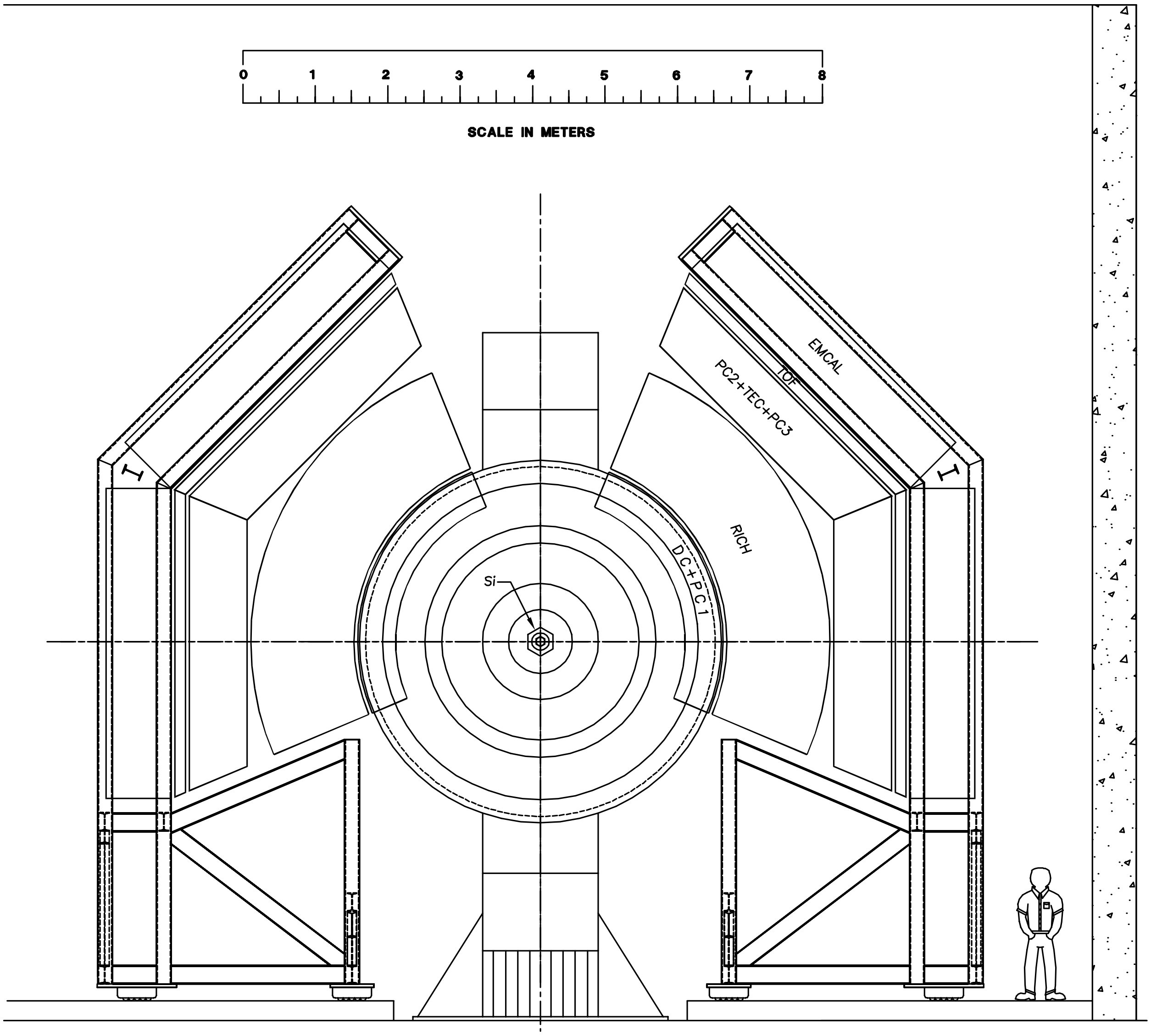

Figure 2.1: Cross-section of the detector through the nominal collision point, showing the layout of detector subsystems in the central arms.

detector only the outer set of coils is installed. The inner set would be added later, together with a detector optimized for rejection of Dalitz decays of π^0's, as discussed in Chapter 15.

Tracking detectors for pattern recognition and momentum measurement of charged particles are arranged in two groups, at $r \approx 2$m (in the fringe field of CM) and at $r \approx 4.5$m. The inner group consists of a multilayer drift chamber (DC) and an interpolating pad chamber (PC1). The outer group consists of a multilayer time expansion chamber (TEC) surrounded by two more pad chambers (PC2 and PC3). The TEC is designed to have six active layers and to be able to detect transition radiation photons as well as charged particles. In the

Baseline configuration the TEC consists of four instrumented layers and does not have transition radiation detection capabilities. The Baseline detector tracking subsystem is described in Chapter 6, and the upgrade of the TEC to its full capabilities is described in Chapter 15.

2.3.2 Electron and Photon Energy Measurements

The electromagnetic energy measurement is accomplished with an integrated calorimeter (EMCal) subsystem at the outer radius of the central arms. The EMCal consists of three components, lead-scintillator (PbSc) sampling calorimeter modules, lead-glass (PbGl) counters, and high resolution crystal (HRX) scintillators. The PbSc and PbGl components are implemented in the Baseline detector and are described in Chapter 9. The HRX is a planned upgrade for PHENIX and is presented in Chapter 15.

The bulk of the approximately 2-sr aperture in the central arms is instrumented with PbSc modules. The remaining portion (25%) is covered with existing PbGl counters. These detectors have comparable energy and time resolution, although a PbGl block has better segmentation (4×4 cm^2) than a PbSc module (5.2×5.2 cm^2). The PbGl array is important for better low p_T γ detection. The PbSc and PbGl counters are expected to play a major role in electron and photon identification, by E-p matching for electrons, and shower shape and timing for electrons and photons. The HRX is expected to improve low p_T single photon detection capabilities.

2.3.3 Particle Identification

The central arms contain a number of detectors for electron and hadron identification. Electron detection at RHIC requires a very good separation of electrons from hadrons over a wide range of momenta (0.2–5.0 GeV/c or greater). This requires that several different technologies, including the EMCal described above, be used in conjunction, both for redundancy and dynamic range. The useful momentum range of each detector used for electron and hadron identification is shown in Table 2.2.

• **Time-of-Flight.** Charged hadrons are measured over a large momentum range with an array of high resolution time-of-flight scintillators (TOF), which can separate pions and kaons up to a momentum of 2.4 GeV/c. The TOF covers one-third of one central arm (~ 0.36 sr). The TOF subsystem is described in Chapter 8. The time resolution of the EMCal ($\sigma_t \approx 300$ ps) is used in the identification of electrons $p \leq 0.35$ GeV/c)(and low momentum hadrons ($p \leq 1$ GeV/c). The excellent timing capabilities of PbSc are an important new feature of the PHENIX calorimeter.

• **Cherenkov Counter.** The central arms each contain a ring-imaging Cherenkov counter (RICH). The RICH is positioned in radius between the inner and outer groups of tracking detectors. The RICH is read out with photomultiplier tube (PMT) array in the Baseline detector. As described in Chapter 7, there is on-going R&D effort to develop a readout based on a parallel-plate avalanche counter with cathode pads and a solid CsI photocathode. Such a readout system might eventually be less expensive than a PMT-based readout. An essentially similar readout technology is being studied for a hadron-blind detec-

Table 2.3: Baseline Configuration: Muon Arm Detectors

Element	Longitudinal Space (mm)	Channel Count	Function
μT	1850–2000, 4000–4300, 6000–6300	19,680	Tracking and momentum measurement.
μID	6600–9150	4608	Muon identification.

tor (HBD) that might serve as an inner tracker for Dalitz rejection. The HBD is a possible upgrade for PHENIX and is presented in Chapter 15.

• **Time Expansion Chamber.** The TEC measures track position and energy deposition along the track. As mentioned above, it will eventually be able to identify electrons by transition radiation detection (TRD). In the Baseline configuration, the TEC is able to identify electrons up to $p_T \approx 2$ GeV/c by measuring dE/dx. The TEC measurement is aided by the PbSc time-of-flight measurement, which is used to eliminate kaons up to 1 GeV/c to allow a comparison of dE/dx between electrons and pions. The electron identification capability of the TEC is complementary to TRD and is retained after the upgrade. Electron identification by dE/dx is independent of the RICH and, like the RICH, operates well in the bulk of the pion p_T spectrum.

2.4 Muon Arm

The muon arm contains detector elements that perform the functions of charged particle tracking and momentum analysis, and muon identification. Table 2.3 summarizes the function and location of these elements, which are also shown in Fig. 2.2.

Particles emerging from the collision point in the polar angle range $10° \leq \theta \leq 35°$ pass through the pole tip of CM. Those which emerge from the pole tip enter the muon arm. The muon arm momentum measurement uses the radial field produced by the muon magnet (MM). The trajectories are measured in multilayer drift chambers (μT) that are arranged in three stations, located at the entrance to, in the middle of, and at the end of the MM field.

Downstream of the MM, muons are distinguished from pions and other shower products by means of a muon identifier (μID), consisting of concrete absorber walls interleaved with planes of limited streamer tubes with cathode pad readouts.

The technical details of the muon arm are presented in Chapters 4 (MM) and 10 (Muon Arm). In the Baseline detector the MM coil and the upper half of the MM "lampshade," as well as the active elements of μT and μID are deferred. This was done for *purely budgetary* reasons. Completion of the muon arm is not regarded as an upgrade, but, if fiscally possible, as part of the Baseline detector intended for Day-1 operation at RHIC. Consequently, in the Baseline configuration certain elements of the muon arm are included whose later installation

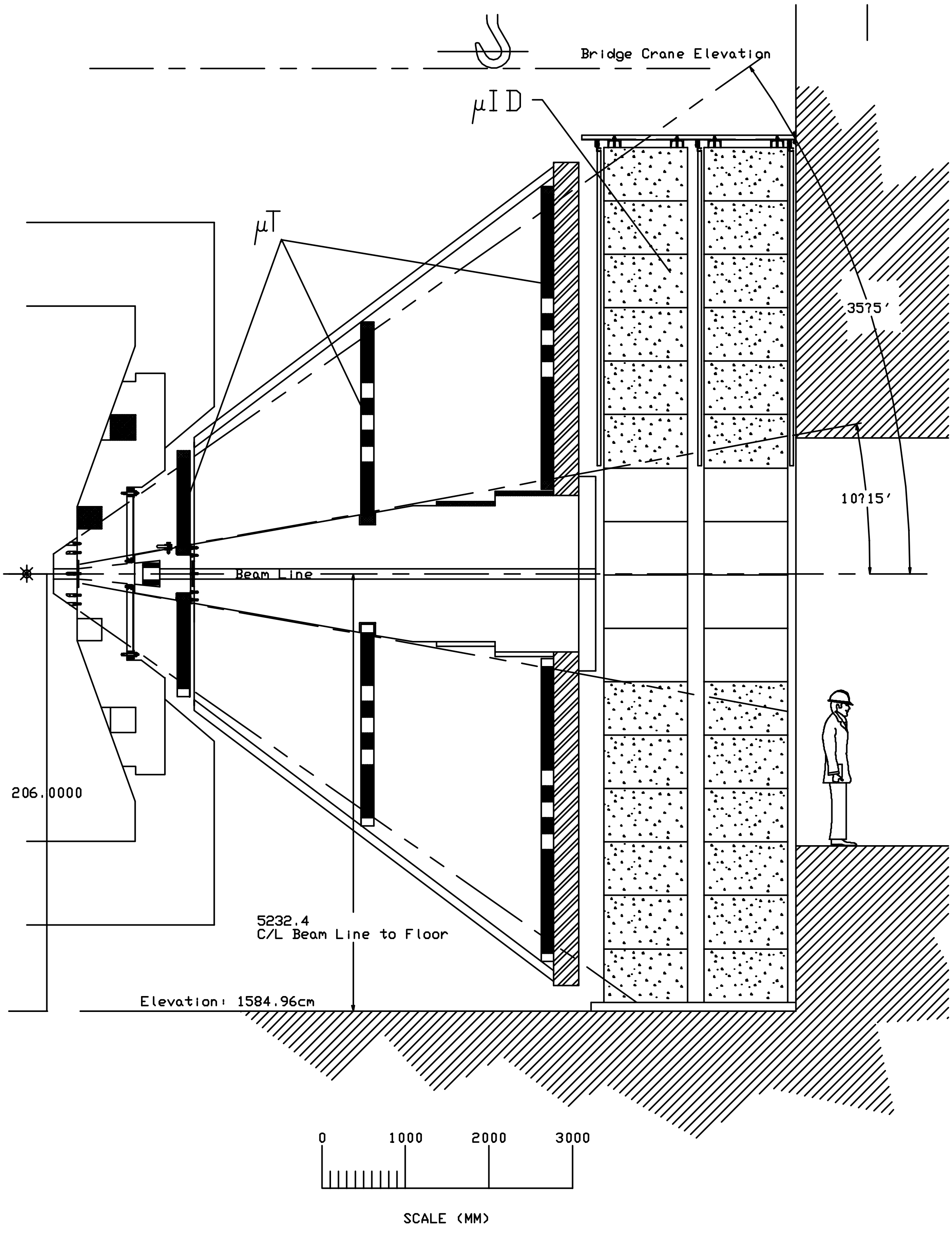

Figure 2.2: Cross-section showing the layout of detectors in the muon arm.

Table 2.4: Baseline Configuration: Inner Detectors

Element	Location (mm)	Channel Count	Function
MVD	$50 < r < 120$ $-350 < z < 350$	43008	Event multiplicity, multiplicity distributions, and precise vertex.
BB	$1750 < \|z\| < 2000$	132	Start time and fast vertex.

would require a lengthy interruption of the PHENIX and RHIC experimental programs. These elements are the MM support structure, the lower half of the lampshade, the endplate, and the conical core (or piston), as well as the μID concrete absorber walls. Efforts are underway to secure additional funds to complete muon arm fabrication and installation with the rest of the Baseline detector. If these funds are not available in time, the proposed strategy will allow for the completion of the muon arm in a normal annual RHIC shutdown period.

2.5 Inner Detectors

The inner detector subsystem consists of detector elements that measure the start time and vertex location of an event, and the event multiplicity and multiplicity distribution. Table 2.4 summarizes the features of this subsystem, which is described in detail in Chapter 5.

Two arrays of beam-beam (BB) Cherenkov counters are located upstream and downstream of the collision point, just beyond the CM poletips. These two arrays are used in coincidence to provide a rough vertex location ($\sigma_z \approx 2$cm) and a precise start time ($\sigma_t < 100$ps) for the event. These counters have a "flashlight" type geometry and cover a pseudorapidity interval $3.1 \leq |\eta| \leq 4$.

The collision point is surrounded by a silicon detector (MVD) array, which covers $-2.7 \leq \eta \leq 2.7$ at a vertex position of $z = 0$ and all of ϕ. The MVD array consists of a two-layer "barrel" plus two one-layer "endcaps." The barrel elements are strips with 200-μm pitch. The endcaps are instrumented with pads. The MVD measures total multiplicity, N, as well as $d^2N/d\eta d\phi$. The MVD also provides a precise ($\sigma_z < 500$ μm) vertex location.

2.6 Trigger and Data Acquisition

The electronics for the PHENIX experiment deal with signals coming from a variety of different detectors, apply selective level-1 (LVL-1) and level-2 (LVL-2) triggers to the data stream, and, because of the large event size and high luminosity, acquire data at a very high rate. The front-end electronics are described in the chapters dealing with the individual detector subsystems. The hardware and software for triggering and data acquisition are described in Chapter 11. The Baseline configuration is briefly described below.

2.6.1 Front-end Electronics

Although PHENIX contains a number of different detector technologies, a strong effort was made in the design of the front-end electronics (FEE) to minimize the number of different types of electronics chains. Reasonable success was achieved in this effort, although it is not possible to digitize all signals in real time directly on the detectors, for reasons of cost and power consumption, for all subsystems. Digitizing in real time of all signals is possible for BB, DC, TEC, and μT, but not for MVD (power/heat), or for RICH, PC, TOF, EMCal, and μID (cost). Consequently, digitized output is stored in Digital Memory Units (DMU) for the first group, and in one of at most three types of switched-capacitor Analog Memory Units (AMU) for the second group. Digitization of the data in the AMU is done, following an "accept" from the LVL-1 trigger, in a local ADC servicing a channel or group of channels.

Another design goal for the FEE is to include the capability of calibrating every channel, under program control. This feature is included explicitly in the cost estimate.

The readout electronics must perform zero-suppression at the earliest possible stage in order to shrink the data volume, and to reduce the computing power needed to do subtractions and corrections to the data. Zero-suppression reduces the raw data volume by a factor greater than 10 for central Au + Au events and nearly 1000 for p + p events. It occurs after a LVL-1 accept and subsequent conversion. Zero-suppression is performed by pipelined processors leading to the LVL-2 and Event Builder buffers.

2.6.2 Level-1 Trigger

The LVL-1 trigger is deadtimeless to enable PHENIX to examine all beam crossings at the highest available luminosities for physics events. It is synchronized with the machine RF clock and must be "pipelined" to be deadtimeless. In other words, LVL-1 will deliver a trigger decision each beam crossing for a beam crossing occurring a fixed time earlier. Studies of the LVL-1 algorithms indicate that about 25 beam crossings are required for the individual subsystems to provide LVL-1 data, and another 10–15 beam crossings for the global component of LVL-1 to finish. Thus it will take 35–40 beam crossings to make a LVL-1 decision. Data is digitized after the LVL-1 decision and, therefore, buffer space for five or six events is also provided. To provide contingency, we use 64-cell long pipelines. As described in Chapter 11, a design for the LVL-1 trigger was made that uses input from BB, MVD, TOF, RICH, EMCal, and μID.

The global LVL-1 decision brings together all subsystem logical primitives. A routing network is included to provide freedom in grouping the input data bits. A series of cascaded lookup tables and programmable scaledown units provides the final LVL-1 decision.

The LVL-1 trigger also provides several thousand pointers to detector elements satisfying certain conditions. These are passed as data to the LVL-2 trigger in order to steer the computational loops at that trigger level.

2.6.3 Level-2 Trigger

The LVL-2 trigger is also a pipelined, however now event-driven, process. It is expected that completion of the LVL-2 algorithms will take much longer than the time between accepted events. Typical processing by the LVL-2 trigger includes the following steps: (1) additional computation at the subsystem level (e.g., application of corrections to get improved primitives for time-of-flight, calorimeter energy clusters, track segment direction cosines, or vertex location); (2) a number of algorithms, presumably running simultaneously on parallel processors, to generate higher-level primitives (e.g., e^-, μ^-, K^-, and γ identification and momentum determination); and (3) global LVL-2 merger of the relevant primitives to produce event signatures (e.g., "e^+e^- pair" or "high p_T photon" or "hadron pair with $\Delta Q < 100$MeV/c").

For the Baseline configuration described here, the LVL-2 trigger is deferred in the same way as the inner CM coils and parts of the Muon Arm. The deferral of the LVL-2 trigger selectivity is consistent with the expected demands on the data acquisition system during early operations at RHIC. The overall trigger and data acquisition architecture is designed to accomodate the LVL-2 trigger, and increased bandwidth at all levels, as required by the design luminosity and future enhanced luminosity. However, implementation of the LVL-2 trigger is expected as soon as additional funding permits. This is motivated by the importance of gaining experience with the LVL-2 hardware and algorithms well before letting them take over the direction of the data collection.

2.6.4 Event Builder and Data Archiving

By the parallel nature of processing in the trigger, accepted events must be assembled from subevents in an "event builder". The event builder must assemble the correct subevents in a robust and reliable fashion. It must also allow expansion on both the input and output sides to accomodate higher rates. This requires handling a higher degree of parallelism on the trigger side and a larger number of output streams on the data logging side. The presently favored architecture is similar to the $N \times M$ matrix employed by E791 at Fermilab. It is easily scaled up for higher throughput. The output streams for PHENIX include banks of processors for global trigger decisions.

The baseline data acquisition system will archive data at 20MB/s. At design luminosities, this rate can keep up with the 2% most central Au + Au collisions and with p + p collisions, although not with p + A and some lighter ion A + A minimum-bias collisions. Thus in early running, or until RHIC reaches the design luminosity, the data acquisition system will be able to collect data with this taping capability and without the LVL-2 trigger. The bandwidth of the entire system, including the implementation of LVL-2, will increase to keep up with expected increases in rates.

Contents